SPUTTERING DEPOSITION OF FERROELECTRIC THIN FILMS AND HETEROSTRUCTURES

Pedro Prieto*[1,2], and Wilson Lopera[1,2]

[1] Excellence Center for Novel Materials, Universidad del Valle, Calle 13 No. 100 - 00, Cali, Colombia

[2] Thin Film Group, Depto. Física, Universidad del Valle, A.A. 25360 Cali, Colombia

Recibido Nov-2006, **revisado** Mar-2007, **aceptado** Jun-2007 **Publicado** Dic-2007

Resumen. La investigación en ciencia básica o aplicada de películas delgadas cerámicas es un campo bastante amplio debido a la posibilidad de desarrollar una nueva generación de pequeños dispositivos a escala micrométrica basados en las propiedades de estos materiales, tales como: permitividad dieléctrica, ferroelectricidad, piezoelectricidad, y piroelectricidad. El reciente crecimiento de la investigación en películas ferroeléctricas ha permitido el desarrollo de nuevas técnicas de deposición de películas y un mejor entendimiento de la ciencia de estos materiales, además de su implementación en forma de películas delgadas en novedosos dispositivos. Este trabajo se enfoca en la síntesis de películas delgadas ferroeléctricas y heteroestructuras usando la técnica de magnetrón sputtering. Se ha desarrollado un sistema de sputtering a alta presión que permite la deposición "*in situ*" de óxidos: superconductors, conductores, magnéticos y aislantes, en una atmósfera de oxígeno. Se ha depositado exitosamente películas epitaxiales de alta calidad del material ferroeléctrico $Pb(Zr_xTi_{1-x})O_3$ mejor conocido como PZT, en estructuras tipo capacitor con $YBa_2Cu_3O_{7-x}$ y $SrRuO_3$ como electrodos metálicos mostrando una reducción del fenómeno de fatiga en comparación con los capacitores basados en electrodos metálicos de Platino.

Abstract. Basic and applied science of ceramic thin films is an extensive research field due to the possibility of developing a new generation of advanced micro-devices that avail from the electronic properties of these materials, like large dielectric *permitivity*, ferro-electricity, piezoelectricity, and pyro-electricity. The recent growth of research on ferroelectric thin films has resulted in the development of new film deposition techniques and a substantial improvement in the understanding of related materials science and implementation of films in various novel devices. This work focuses on the synthesis of ferroelectric thin films and heterostructures by using the magnetron sputtering method. We have developed a high pressure sputtering technique that permits the "*in situ*" deposition of superconducting, conducting, magnetic, and insulating oxides in an atmosphere of oxygen. We have successfully deposited high quality epitaxial thin films of ferroelectric $Pb(Zr_xTi_{1-x})O_3$ known as PZT, in capacitor structures with $YBa_2Cu_3O_{7-x}$ and $SrRuO_3$ conducting electrodes showing a reduced polarization fatigue in comparison to capacitors using metallic-Platinum electrodes.

1 Introduction

Different vapor-phase deposition techniques such as Plasma Sputtering Deposition (PSD), Ion beam deposition sputter deposition (IBSD), Laser Ablation Deposition (LAD), electron beam or thermal evaporation for Molecular Beam Epitaxy (MBE), and Chemical vapor deposition have been applied to produce ferroelectric films and layered heterostructures. See reference [1] for a review on these techniques. This work focuses on the synthesis of ferroelectric thin films and heterostructures by using the magnetron

sputtering method. We have developed a high pressure sputtering technique that permits the "*In Situ*" deposition of superconducting, conducting, magnetic, and insulating oxides in an atmosphere of oxygen that avoid the re-sputtering problem that appears in conventional commercial sputtering systems. This method has been successfully used for the deposition of high quality epitaxial HT_C thin films and is now being used for the in situ deposition of $Pb(Zr_xTi_{1-x})O_3$ known as PZT, in capacitor structures with $YBa_2Cu_3O_{7-x}$ and $SrRuO_3$ conducting electrodes showing a reduced polarization fatigue in comparison to capacitors using metallic-Platinum electrodes.

2 Thin Film Ferroelectric Materials

Most of the applications of ferroelectric materials like FEDRAM, IR sensors, and FEFET transistors demand the deposition of these materials as a thin film in between two conductive electrodes in a capacitor geometry. Fig. 1 shows different types of devices that can be produced by using ferroelectric thin films [2]. The marriage of ferroelectric thin film technology with silicon-based technology offers the potential of combining non volatility with fast read/write characteristics along with the small cell size of DRAM. It should be noted that new materials and additional process steps will have to be implemented in the standard IC processing environment. The highest density is obtained with the memory cell having one transistor and one capacitor (1T/1C cell), as shown in Fig. 2.

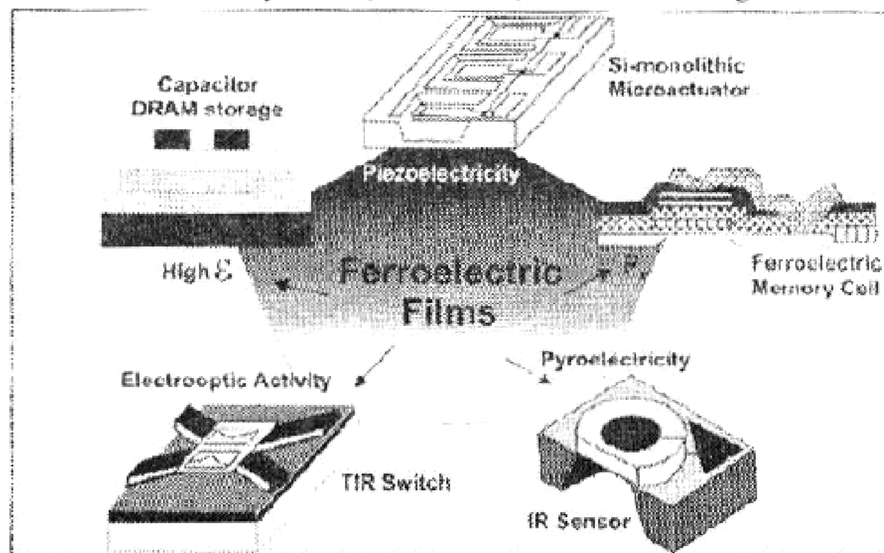

Fig. 1 Selected applications of ferroelectric thin films in micro-devices.

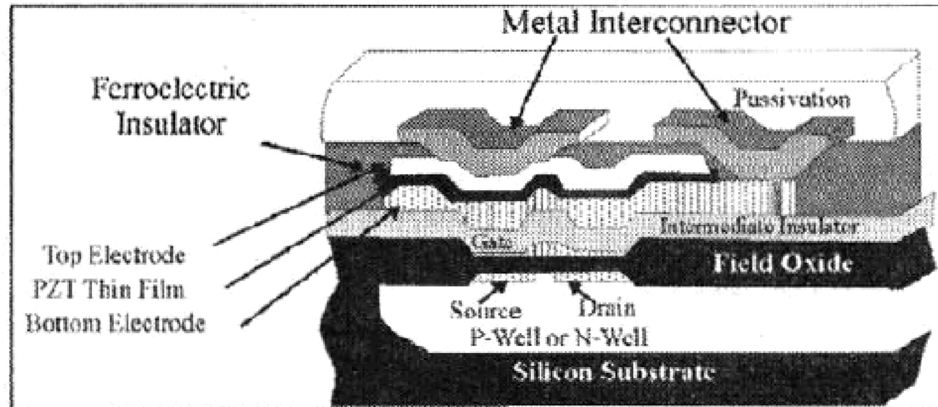

Fig. 2 Schematic view of a FEDRAM.

The most promising materials for Ferroelectric Random Access Memories, FEDRAM applications are lead zirconate-titanate, $Pb(Zr_xTi_{1-x}O_3$ (PZT) and strontium bismuth tantalite, Sr_2BiTa_2O (SBT). Both of these materials have a perovskite-layered structure as shown in figure 3.

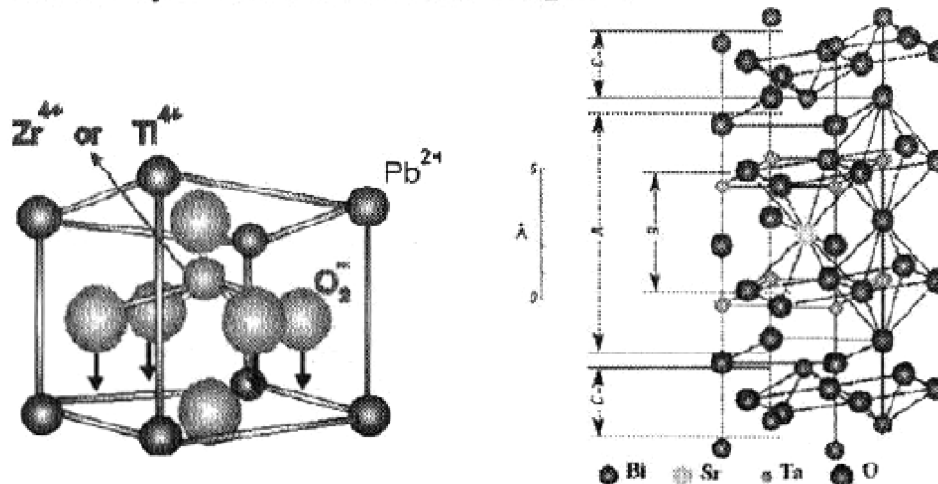

Fig. 3 (a) Crystal structure of PZT (b) Perovskite Structure of SBT.

PZT is a solid solution of lead zirconate ($PbZrO_3$) and lead titanate ($PbTiO_3$) that crystallizes in the perovskite structure like the crystal structure of $BaTiO_3$. Depending on the ratio of Ti/Zr, the crystal structure and the properties can be tuned. At the morphotropic phase boundary (x=0.53), independent of temperature, see Fig. 4, the rhombohedral and tetragonal phases coexist. In bulk ceramic, the strongest piezoelectric behavior is observed at the morphotropic phase boundary, making this composition interesting for piezoelectric applications [3]. For ferroelectric memory

applications Ti-rich (tetragonal) compositions usually provide higher polarization values. For pure $PbTiO_3$ oxide a spontaneous polarization of 81 mC/cm^2 was calculated from the ionic displacements. With increasing Zr content (x = 0.4) Ps decreases to a value of 65 mC/cm^2 [4].

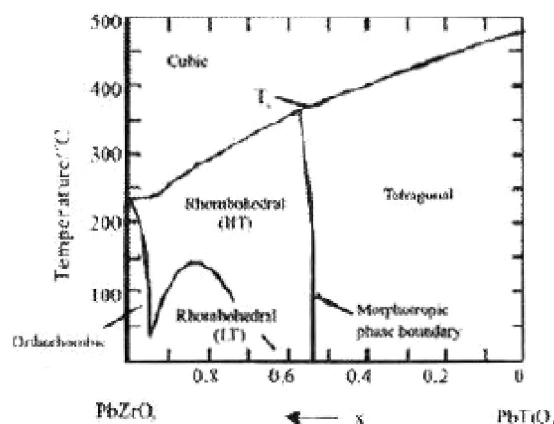

Fig. 4 Phase Diagram of PZT .

4SBT belongs to the Bi-layered compounds of the Aurivillius type ABi_2B_2O. The tetragonal crystal structure above T_C is shown in fig 3b. SBT consists of perovskite building blocks of TaO6 octahedral separated by bismuth oxide planes ($Bi_2O_3^{2+}$). SBT exhibits two phase transitions at approximately 310^0 C and 570^0 C [5]. Upon cooling below the upper transition temperature, the symmetry changes to an orthorhombic, ferroelectric phase resulting in large distortions in both, bismuth oxide layers and perovskite sheet. At the lower transition, there is no change of symmetry; however, a sizable change in the spontaneous polarization takes place. There is still a discussion on the ferroelectric state of SBT. Recent studies suggest that besides the Ta-O distortion, a displacement of the Bi and oxygen ions in the $Bi_2O_2^{2+}$ layer contributes a significant part to the spontaneous polarization in SBT. The value of P_s ranges between 14 and 18 mC/cm^2. However, it is agreed that the spontaneous polarization can only be switched in the a-b plane, and not in the c-direction [6] (see Fig.3b). In SBT thin films, the coercive field, as well as the remnant polarization are significantly smaller compared to PZT (fig. 5). By measuring the hysteretic loops of thin films with a thickness of 140 nm, typical values for tetragonal PZT and SBT were found: V_c = 12 V,

P_r= 30 mC/cm^2 (for PZT) and V_c = 0.6V, P_r = 10 mC/m^2 (for SBT). In practice, one finds mostly lower values of polarization and higher coercive fields for thin films.

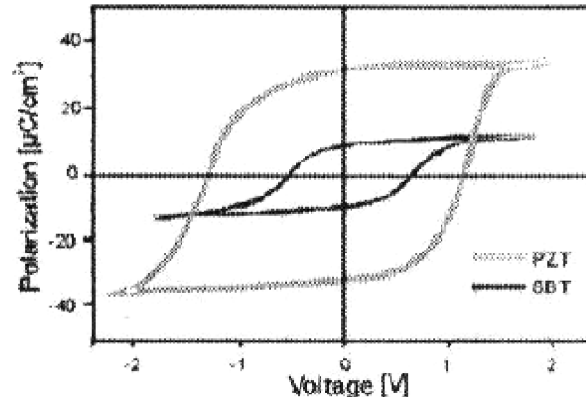

Fig 5 Comparison between hysteretic loops of $Pb(Zr_{0.3}Ti_{0.7})O_3$ and SBT thin films with a thickness of 140 nm.

The decision on the best choice is still under discussion. Besides the ferroelectric properties, the compatibility to the silicon CMOS technology, the endurance of the ferroelectric capacitor, as well as the device concept, all play decisive roles. For DRAM applications, a low coercive voltage of the ferroelectric capacitor is required. In a first approach, this could be carried out by reducing the film thickness; however, it should be taken into account that by decreasing the film thicknesses the coercive field is enhanced and the remnant polarization is reduced. Thus, for each individual case, the thickness scaling has to be verified with respect to the figure of merit, which is illustrated in fig. 6. From these results, it is obvious that thin films of PZT 20/80 are rather suitable for low voltage application than are thin films of PZT 35/65. The thickness dependence of the coercive field, as well as the switching properties in ferroelectric thin films has been explained by the assumption of the existence of a (non-ferroelectric) layer at the interface between the electrodes and the film, e.g. [7].

The electrical properties of the interface layer differ from those of the film. Under an electrical field, charges are injected through a surface dielectric layer resulting in a change of the switching behavior [8,9].

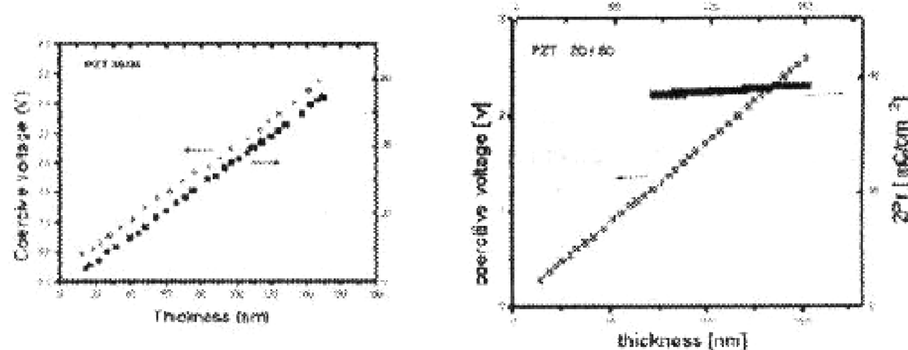

Fig. 6 Thickness dependence of coercive voltage and ΔP of PZT thin films with compositions: $Pb(Zr_{0.35}Ti_{0.65})O_3$ and $Pb(Zr_{0.2}Ti_{0.8})O_3$.

3 Orientation of Ferroelectric thin films

In standard systems for ferroelectric thin films, e.g. PZT with platinum electrodes on an oxidized silicon wafer and the measured remnant polarization is only about half of the spontaneous polarization; the reason is the orientation of the crystallographic axes of PZT in the (111)-direction. In addition, ferroelectric domains, which can still exist after a poling process prevent a complete switching of the spontaneous polarization. Ferroelectric thin films are typically crystallized at high temperatures (about 700 ºC). The growth of the ferroelectric film on the substrate is favored in that orientation delivering the best match of substrate and thin film. Due to the different thermal expansion coefficients, the subsequent cooling results in elastic stresses on the interface (either compressive or tensile, due to the lattice mismatch). Crossing the ferroelectric phase transition evokes, besides the spontaneous polarization, a spontaneous deformation of the lattice cell. Assuming a tetragonal structure of the ferroelectric film and a compressive stress by the substrate, the c-axis of the distorted cell is predominantly oriented perpendicular to the surface (001). For tensile stress, the a-axis is favored perpendicular to the surface (100) [10]. Because of the "clamping" conditions by the substrate, the ferroelectric thin films suffer elastic stress. In order to reduce this stress (as well as electrical stray field energy) ferroelectric thin films are driven to split into domains. Notice that lowering the elastic energy requires the formation of non-180º-domain walls between adjacent domains, i.e. 90º (for tetragonal structures) or 71º and 109º (for rhombohedral structures), whereas electrical energy is already reduced by forming 180º-domains.

The process is quite similar to bulk ceramics where each grain is mechanically clamped by its surrounding neighbors [11].

In Fig. 7 possible domain patterns of different textures of tetragonal film are depicted. For (001)-oriented PZT, which was prepared by deposition on magnesium oxide substrates causing compressive stress, 90^0 as well as 180^0-domains are expected. Under the influence of an electric field the number of 180^0-domains is decreased.
The resulting pattern predominantly consists of 90^0-domains. Notice that the polarization is arranged in a "head-tail" configuration to avoid discontinuities in the polarization (div P = ñ). A (100)-orientation of PZT is realized by using a buffer layer of yttrium-stabilized zirconium and an oxide electrode of lanthanum strontium cobaltate.

The change of domain structure by poling is similar to the (001)-orientation, but the a-axis orientation is still preferred. In (111)-oriented PZT, poling will evoke the single domain state while the "head-tail" configuration is required. However, there is still discussion on whether the 90^0-domain walls are generally mobile.

It is known from research on ferroelectric thin films that coercive voltage in thin films also depends on the excitation signal frequency [12]. The dependence is more pronounced in SBT than in PZT thin films, as illustrated in fig. 8. Increasing the cycle frequency could lead to a reduction of the remnant polarization because the coercive field becomes equal to the operating voltage and the switching process is incomplete. However, more detailed investigations show that a different mechanism from the nucleation of domains and their kinetics might be decisive for the polarization switching, even though the characteristic frequency dependence of E_c is observed. Lohse [13] found that by applying voltage steps in the order of the coercive voltage, a Curie-von Schweidler behavior is displayed, i.e. $I \; a \; t^{-a}$ during the whole time when the polarization reverses. Thus, switching appears as a polarization process with a broad distribution of relaxation times, which are typical for all electro-ceramic, ferroelectric, as well as dielectric thin films.

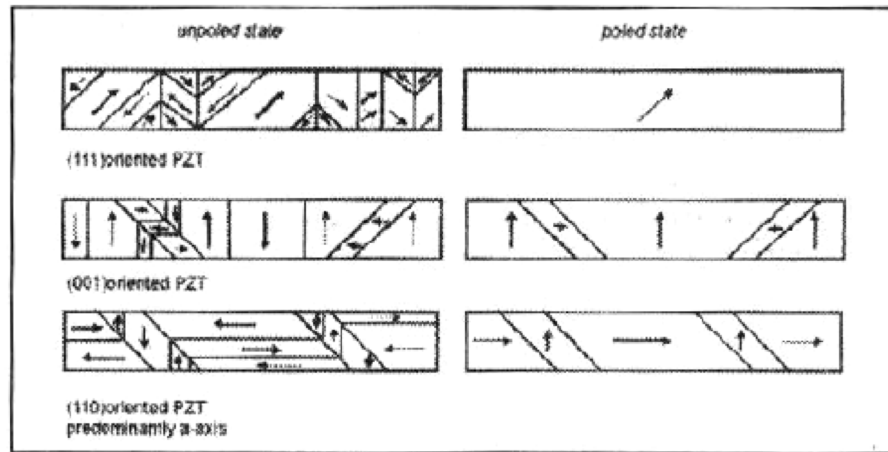

Fig. 7 Domain structure of tetragonal PZT with different orientations.

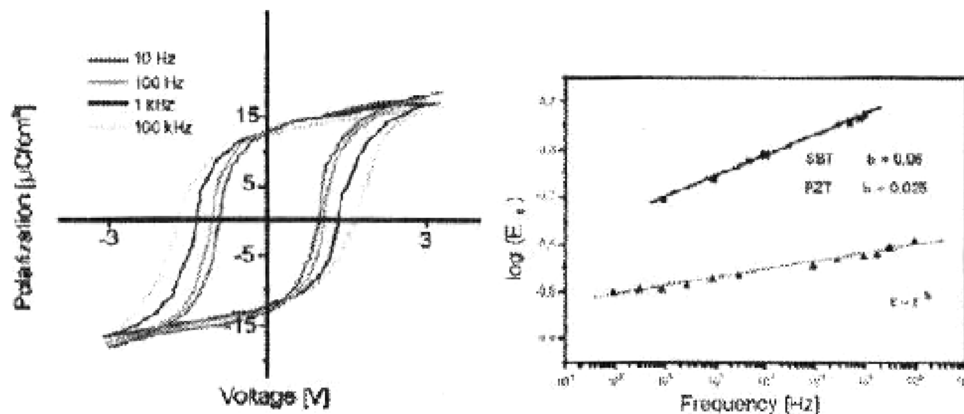

Fig. 8 (a) Frequency dependence of Hysteretic loop of SBT
(b) Coercive field in SBT and PZT 20/80

4Electrodes Platinum electrodes are widely applied in integrated ferroelectric capacitors. They are normally deposited by sputtering. For the case of bottom electrodes on an oxidized silicon wafer Pt is used along with a thin Ti (or Ta) film acting as an adhesion promotor. The thickness of the Pt and Ti films are typically 70 – 200 nm and 5 – 10 nm, respectively, when the Pt bottom electrodes are annealed in an oxygen ambient or are heated after deposition of PZT, hillocks are formed at the surface. In addiction, the Ti adhesion films are oxidized to TiO [14]. Both processes have to be limited to avoid both short-circuiting and the possible formation of non-ferroelectric interface films. This can be done by reducing the thickness of the Pt and Ti layers as much as possible while maintaining a

good adhesion and pinhole-free layers. Good results with relatively few and shallow hillocks can be obtained [15]. When imperfections such as pinholes are present in the Pt film, the PZT can react with the underlying SiO or silicon and lead silicates will be formed.

The morphology of the bottom electrode has been found to strongly influence the microstructure of the PZT film. In sol-gel technology, nuclei are necessary to obtain well-crystallized films, and the hillocks can serve as such.

Compared to the bottom electrode, the top electrode is less affected by subsequent processing. This gives more freedom in the selection of top electrode material. However, for FEDRAM applications a symmetry in the two switching directions is required, so for this reason the use of the same material (e.g. Pt or Ru) for both top and bottom electrodes is strongly preferred. Furthermore, it has been found that a rapid thermal anneal after deposition of the top electrode to a temperature higher than T_c improves the ferroelectric properties. This can be ascribed to stress related effects [16].

Pt/PZT/Pt structures satisfy many of the demanding requirements for high-density non-volatile memories. The main problems are encountered with the controlling and minimizing of the fatigue of these capacitors. In this respect any or all routes can be followed: (1) optimizing the properties of the Pt/PZT/Pt stack (i.e. interface control), (2) using alternative electrodes, and (3) using other ferroelectric materials.

Recently it has been reported that low-fatigue capacitors can be fabricated using layered ferroelectric materials deposited with sol-gel and with Pt electrodes [17]. One example is the system $SrBi_2(Ta, Nb)_2O_8$ [18]. Results on the endurance indicate that in such materials the fatigue is substantially less than in PZT; published experimental data show switching up to 10^{12} cycles. However, polarization values reported are significantly smaller (P_r ~ $6mC/cm^2$) than those for PZT [19].

As alternative electrode materials (di) oxides of (noble) transition metals such as Ru, Ir, and Os that combine a low resistivity with a high thermal stability have been used. Their bulk resistance ranges from 30 - 100 mW.cm.

Besides the oxides, the metals themselves can also be used as electrodes for ferroelectric materials, either in the elemental state or as alloys. As a consequence, a number of different combinations of the noble transition metals and their oxides have been used in ferroelectric capacitor structures. RuO_2 is the most widely applied. For PZT with RuO_2 electrodes, the fatigue is much improved compared to PZT with Pt electrodes. Recently it has been reported that IrO_2 shows similar properties [20].

The formation of a second phase, presumably $PbRuO_3$ at the PZT grain boundaries has been observed. This is probably the cause of the significantly higher conductance of PZT deposited on RuO_2 as compared to comparable PZT deposited on Pt electrodes. The conductive oxide electrodes are generally prepared by reactive sputter deposition.

5 Deposition methods for Ferroelectric materials

Deposition techniques for complex oxide materials which are also viable for large-scale device fabrication include sputter-deposition [21], spin-coating sol gel [22], and organ metallic CVD (OMCVD) [23]. With these methods one is capable of fabricating homogeneous films over wafer memories with 150-200 mm diameter having thicknesses in the range of interest for ferroelectric memories (0.1-.04 mm). Although sputtering is applied for preparation of PZT in the first commercial non-volatile memory [24], the methods of spin-coating and chemical vapor deposition (CVD) are currently more broadly applied.

If one compares the deposition of large-area PZT films by methods of sputtering, sol-gel, and OMCVD, the greatest efforts in recent years have been directed towards sol-gel technique. This situation is changing; efforts are increasing on OMCVD methods. However, the continuous deposition at a temperature where the PZT phase is directly formed, leads to very homogeneous and reproducible films having very good ferroelectric properties. This, together with the acceptable (conformal) step coverage, explains the increased interest in this method. The sol-gel technique's advantage is that it is a simple processing technology, which does not require very expensive apparatus. This means that on a substrate with topography variations there are also film thickness variations, this can result in etching problems causing difficulties in device production.

The sputtering method, is now a very attractive method for preparing heterostructure oxide films, the requirement of high-oxygen partial pressures during the deposition has been solved by using high-pressure processes at high temperatures, as will be described in section 7.

6 Sputtering Deposition

The simplest sputtering system is the so-called DC-sputtering, which is schematically shown in Fig. 9a. In a vacuum chamber the target material, which is eroded, is at the cathode side (negative potential), and the substrate for the film is located at the anode side. The potential of several hundreds of Volts between these plates leads to the ignition of plasma discharge for the typical pressures of $10^{-1} - 10^{-3}$ mbar and the positively charged ions are accelerated to the target. These accelerated particles sputter off the deposits, which arrive to the substrate mostly as neutral atoms. The discharge is maintained as the accelerated electrons continuously ionize new ions by collisions with the sputter gas. Fig. 9b shows the potential distribution: as the plasma is a good conductor, there is no major potential drop in the plasma region, and, due to the different mobility of electrons and ions, the main voltage drop is observed at the cathode regions (darkroom). This potential distribution is advantageous as the acceleration of the sputtering gas ions proceeds directly in front of the target and not in a region far off, where the ions would undergo additional collisions and loose their energy on a long path to the target.

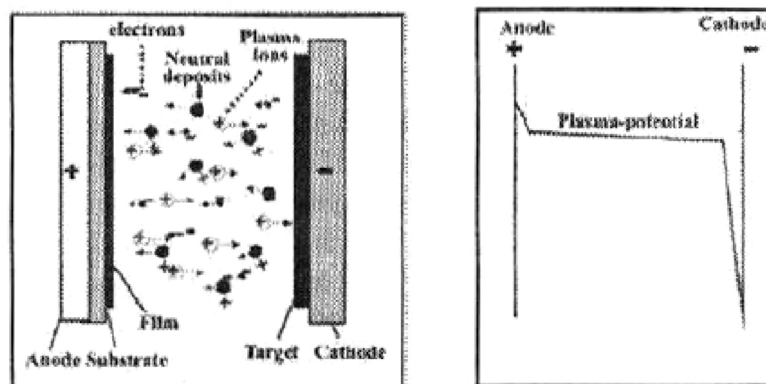

Fig. 9 (a) Schematics of a DC-Sputter system. (b) Potential between anode and Cathode.

The sputtering process is schematically illustrated in fig. 10a. The ion, which has been accelerated within the darkroom, with nearly the full voltage

of 50 to 1000V applied, strike the surface atoms. The following collision cascade leads to a heating of the target and finally, also to some back-reflected atoms which can leave the surface. The details of these collision cascades can be simulated very reliably by molecular dynamic methods, and some results on the sputtering yield, and the dependence of the relative masses of projectile and target atom are shown in Fig. 10b [25]. The threshold energy for sputtering is much higher than the surface binding energy, E_b, of the atoms, which is in the order of 4 to 8 eV. This difference can be directly understood, as several collisions are necessary in order to obtain an atom in backward direction. Hence, the threshold is observed at $4E_b$ to $8E_b$ corresponding to a threshold energy of 20 to 50 eV. A linear increase is observed for many conditions up to voltages of 1000 V. At higher energies the ions penetrate too deeply into the target and the yield decreases again.

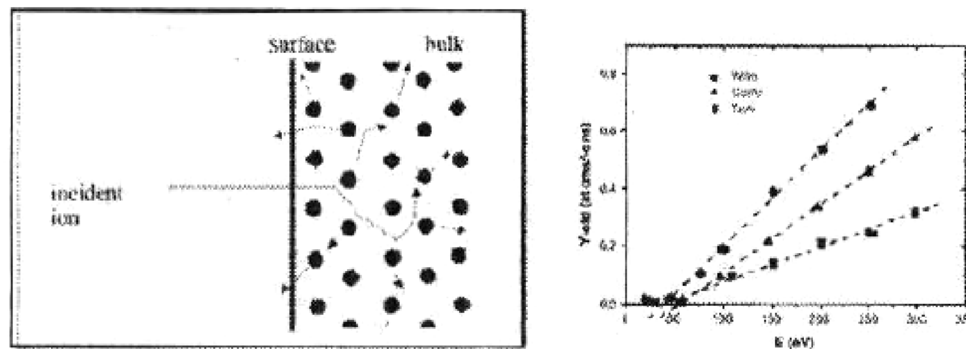

Fig 10 (a) Principle of sputtering by collisions sequence
(b) Dependence of the sputtering yield on ion energy and target composition.

As shown for the example of Co and Ti, different yields are observed for different target atoms and this difference, in principle, yields the deposition of a film of different stoichiometry. However, there is generally a good self-regulating mechanism: due to the very low penetration depth of the sputtering process, the faster eroded component is denuded after a short initial time and finally, in a quasi-equilibrium the difference in yield is compensated by the enrichment. Therefore, sputtering quite generally allows the deposition of films with the same stoichiometry as the target.

An ionization degree of less than 1% of the atoms is characteristic for a plasma and consequently a rather low sputter rate. To improve the ionization rate, magnetic fields can be used forcing the electrons on helical

paths close to the cathode and yielding a much higher ionization probability. A typical arrangement using permanent magnets and the corresponding fields is shown in fig. 11. Additionally, this magnetron arrangement allows for lower gas pressure; however, it has the disadvantage of a more inhomogeneous target erosion than a simple planar geometry.

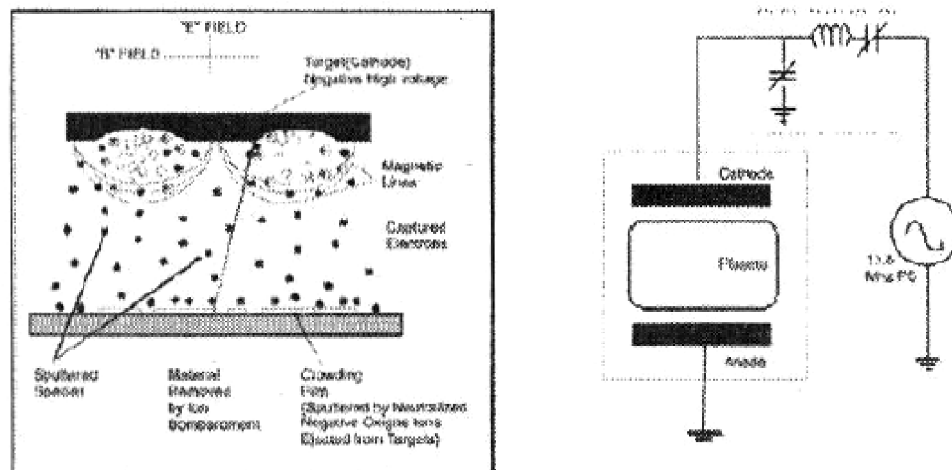

Fig. 11 (a) Schematics of the deposition process in a magnetron sputtering.
(b) RF-plasma sputter system with RF matching network.

DC sputtering works fine as long as the target material has a minimum electrical conductivity; however, there is electric load for insulating targets. This problem can be solved by a high frequency plasma discharge as shown in fig. 11b. A typical frequency of 13.6 MHz is capacitively coupled to the target and there is only a small voltage decay across the electrode. The substrate and the deposition chamber are generally grounded. As the electrons are much faster than ions, a negative potential at the electrodes – as compared to the plasma potential – evolves during each cycle. With a symmetrical arrangement of cathode and anode, we would obtain similar re-sputtering rates, but no film growth; however, non-symmetries are introduced by the capacitive coupling of the RF, which yields some bias voltage and differences in the geometry, e.g. different sizes of target and substrate. Nevertheless, deposition rates are much lower than for DC sputtering.

7 Sputtering Deposition

Compared to the other physical deposition methods, the partial pressure of the sputtering gas is an additional and important process parameter that

must be considered and optimized. This pressure controls the free path length of the atoms and therefore their energy, angular distribution, and, finally, their incorporation into the films.
For oxide layers, the gas pressure is even more important as negative oxygen ions are formed, which can re-sputter from the film. As the re-sputtering yield also depends on the different elements, the stoichiometry of the growing films is changed and these changes of the film are not compensated, as was the case for the sputter yield from the target discussed above. One possibility to reduce the re-sputtering effect is by using the "off-axis" geometry; in this method the substrates are positioned perpendicular to the target on one side to minimize the number of O ions impacting on the growing films. This method is shown in fig. 12 [26]. This system works at a partial oxygen pressure of about 0.1 mbar and an Ar pressure of approximately 0.3 mbar, producing high-quality oxide thin films with the correct stoichiometry, but at very low deposition rates.

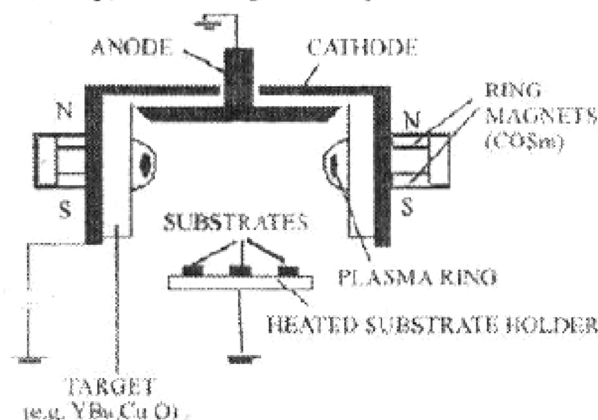

Fig. 12 "Off-axis" sputtering system as per J. Geerk et al. [26].

The re-sputtering can be reduced by the high pressure sputtering method developed by U. Poppe et al [27] in"on-axis" geometry, as shown in fig. 13. With this system it is possible to deposit high-quality oxide thin films in pure oxygen at pressures of about 3-4 mbar, at these pressures the mean free path of the Oxygen ions is some micrometers that conduct to a thermalization of the negative oxygen ions in the space between target and substrates (1-2 cm), reducing the re-sputtering of the deposited material on the substrate by the collision of the negative oxygen ions.
The method permits the deposition of conductive oxides like $YBa_2Cu_3O_7$, $La_{2/3}Ca_{1/3}MnO_3$, and $SrRuO_3$ by using DC and also insulator oxides like SrTiO3, BaTiO3, and $PbZr_xTi_{1-x}O_3$ by using RF sputtering. In the case of

Pb-based perovskite oxides like PZT, the deposition is complicated by the fact that PbO is known as a very volatile oxide.

This vaporization must be considered and controlled in the deposition of the different compounds. Under atmospheric pressure the volatile species is PbO and the vapor pressure of Pb is 3 orders of magnitude lower; in contrast, under UHV conditions, the dominant species in the vapor phase is Pb. The high-pressure sputtering method permits an adequate control of the Pb stoichiometry of the deposited films, due to the high-oxygen pressure used during the deposition.

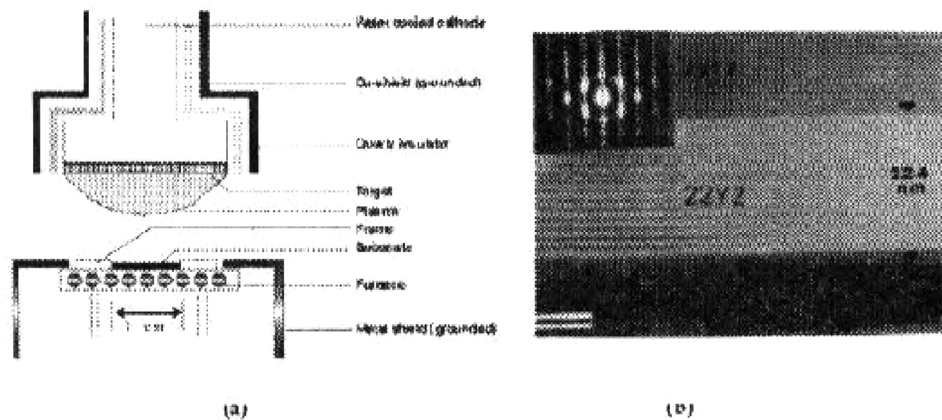

(a) (b)

Fig 13 (a) High-oxygen pressure sputtering system.
(b) HRTEM image of a tri-layer oxide structure deposited *"in-situ"*.

Fig 14: shows a multitarget high-oxygen pressure system operated in DC/RF mode for the "in-situ" deposition of electrically conducting $SrRuO_3$ oxide films and ferroelectric $Pb(Zr_{0.2}Ti_{0.8})O_3$. A perfect control of the interface and the epitaxial growth can be obtained by this rather slow growth process as shown by the cross sectional HRTEM image shown in figure 15 [28]. The sputtering conditions used for the deposition of these heterostructures are summarized in Table 1. Two different electrodes have been employed to obtain the ferroelectric properties of Sputtered PZT films; $YBa_2Cu_3O_7$ and $SrRuO_3$.

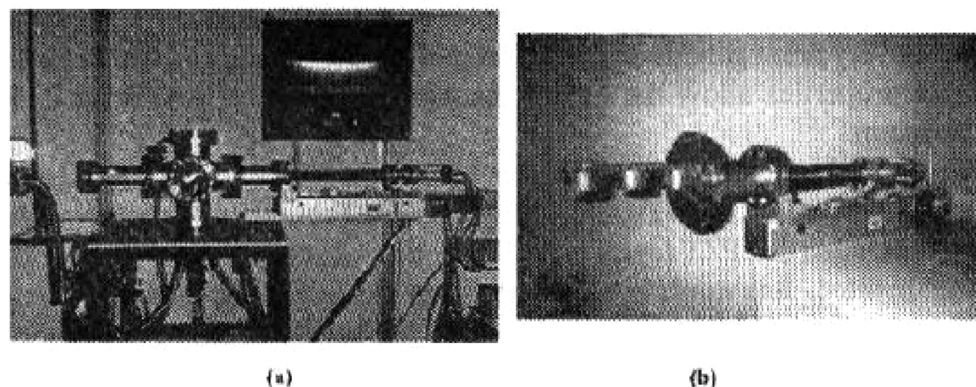

(a) (b)

Fig 14 (a) Multitarget system for the "in-situ" deposition of Oxide heterostructures. (b) Details of the three target holder.

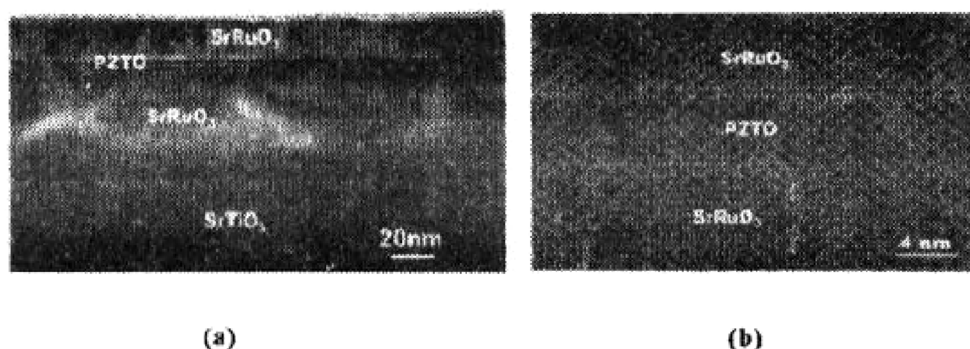

(a) (b)

Fig 15. (a) Low magnification image of SRO/PZT/SRO Tri-layer deposited "in-situ" by high-pressure sputtering method. (b) High resolution TEM image showing the sharp interface in the heterostructure [28].

Table 1 Sputtering condition for the preparation of PZT and SRO thin films.

	$Pb(Zr_xTi_{1-x})O_3$	$SrRuO_3$
Power	RF 80 - 120 W	DC 320 V 150 mA
Targets	$Pb_{1.1}(Zr_{48}Ti_{52})O_3$	$SrRuO_3$
Substrates	$SrTiO_3$, Si/Pt	$SrTiO_3$
Sputtering Gas	O_2 80% Ar 20%	O_2 100%
Gas Pressure	3.5 mbar	3.5 mbar
Substrate temperature	600 °C	600 °C

film is displayed in figure 16. A metallic behavior is observed with a paramagnetic to ferromagnetic transition at about 150 K. The inset shows AFM-measurements of the SRO film. . A Root Mean Square (RMS) roughness of 20 Å was observed for a 100 nm thick SRO film on a STO

(100) substrate. This is a typical value for an area of 4x4im². SEM analysis shows very homogenous and atomically sharp interfaces without defects. these properties allow the use of the SRO as an electrode in a PZT capacitors.

Figure 17 shows the X-ray diffraction pattern for PZT films on YBCO and on SRO deposited on SrTiO3 (001) substrates. From these measurements we concluded that PZT layers grown on both oxide electrodes are highly c-axis oriented. It is worth to explain the identification of the peak at 2q 36.5 degrees in the diffraction pattern of figure 17b. This peak can be reasonably associated with the diffraction of $Ti1_{-x}Zr_xO_y$ with 0.5<x< 0.7, labeled TZO. The coexistence of titanium oxide with lead oxide, TZO, explains the formation of the $Pb(Zr, Ti)O_3$ phase in the sputtering deposition process.

Ferroelectric hysteretic loops and fatigue behaviors were performed using the ferroelectric tester TR66A from Radian technologiesä for STO/YBCO/PZT/Pt and STO/SRO/PZT/SRO capacitor structures, with PZT thicknesses ranging from 50 nm to 150 nm. Well saturated hysteretic loops with good square shapes were observed for PZT on these types of oxide electrodes. The use of SRO as an electrode significantly improves the fatigue behavior, as shown in figure 18.

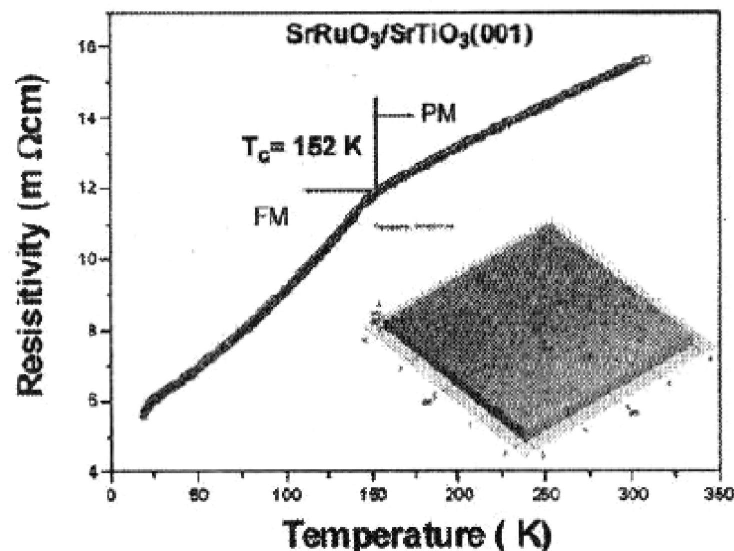

Fig. 16 Resistivity as function of temperature for a sample of $SrRuO_3$. The inset shows the AFM of the film surface.

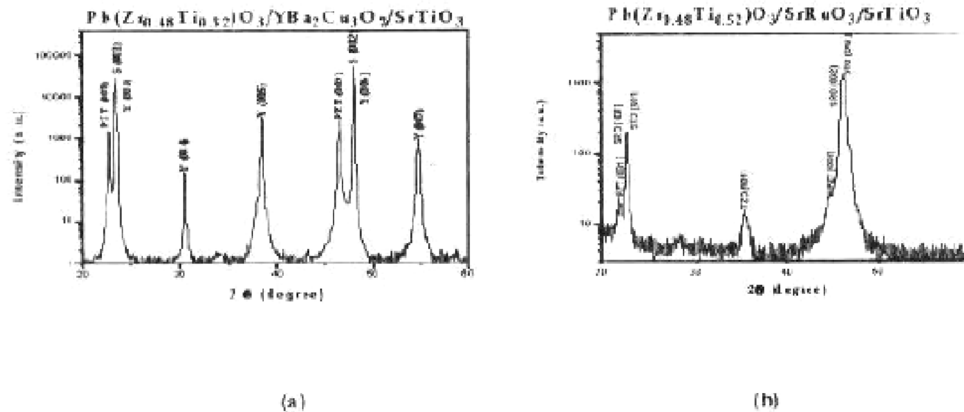

(a) (b)

Figure 17 X-ray Diffraction pattern for **(a)** PZT/YBCO/STO (100) and **(b)** PZT/SRO/STO (100).

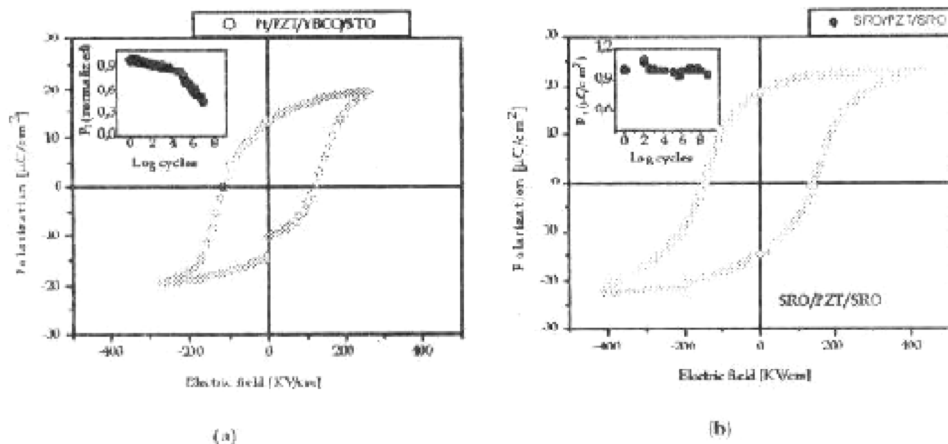

(a) (b)

Fig 18. Polarization hysteretic loops for PZT capacitors deposited on $SrTiO_3$ (001) substrates. **(a)** YBCO/PZT/Pt and **(b)** SRO/PZT/SRO; all measurements were taken at 5 Volts on 250 μm diameter top electrodes.

8 Conclusions

The high-pressure sputtering method has been used for the "*in-situ*" deposition of high-quality PZT thin films on superconducting $YBa_2Cu_3O_7$ and conducting $SrRuO_3$ electrodes on single $SrTiO_3$ at temperatures below 600 °C. Highly c-oriented PZT films with sharp atomic interfaces between the PZT film and the electrodes have been obtained. Remnant polarization values in the range of 10-20 mC/cm² at room temperature for PZT

thicknesses ranging between 50 and 150 nm with improved fatigue behavior have been obtained in these structures.

In summary, highly oriented PZT-based capacitors with YBCO, SRO, and Pt electrodes fabricated on $SrTiO_3$ single crystals display excellent ferroelectric characteristics at room temperature. These properties make these capacitors principal candidates for applications in NVFDRAM devices.

9 Acknowledgements This work has been financed by COLCIENCIAS under the project "*Nanoscale characterization of ferroelectric thin films*" Contract Nº 1106-05-12408

10 References

[1] MRS Bulletin **21** (2) *Electroceramic Thin films Part I Processing* Eds. O. Auciello, and R. Ramesh (1996)

[2] S. B. Krupanidhi; in "*Multicomponent and Multilayered Thin Films for Advanced Microtechnologies: Techniques Fundamentals and Devices*", pag. 601-625, ed. O Auciello and J. Engelmann, Kluwer Academic Publisher (1993)

[3] B. Jaffe, W. R. Cook and H. Jaffe, *Piezoelectric Ceramics*, Academic Press, London (1964)

[4] B. A. Tuttle, J. A. Voigt, D. C. Goodnow, D. L. Lampra, T. J. Headley, M. O. Eatough, G. Zender, R. D. Nasby and S. M. Rodgers, "*Highly oriented chemically prepared $Pb(ZrTi)O_3$ Thin Films*", REVISTA **6**(6) 1537 (1993)

[5] R. E. Newnham, R. W. Wolfe, R. S. Horsey, F. A. Diaz-Colon and M. I. Kay, Mat. Res. Bull., **8** 1183-1195 (1973)

[6] K. Ishikawa and H. Funakubo, Appl. Phys. Lett. **75** (13) 1970-1972 (199X).

[7] W. Klanzig, Phys. Rev. A **98** 549-550 (1955)

[8] J. F. Cilissen, M. W. Prins and R. M. Wolf, J. Appl. Phys. **80** (6) 2777-2783 (1997)

[9] A. K. Tagantsev and L. A. Stolichnov, Appl. Phys. Lett. **74**(9) 1326-1328 (1999)

[10] O. Auciello, H. N. Al-Shareef, K. D. Giord, D. J. Lichtenvalner, R. Dat, K. R. Bellur, A. I. Kingnon and R. Ramesh, Mater. Res. Soc. VOLUMEN 241-353 (1995)

[11] G. Arlt, J. Mat. Sci. **25** 2655-2666 (1990).
[12] J. F. Scott, Int. Ferroelectrics, **12** (2-4) 71-78 (1996).
[13] O. Loshe, M. Grossmann, U. Bolten and R. Waser, J. Appl. Phys. **89** (4) 2332-2336 (2001)
[14] G. A. C. M. Spierings, J. B. A. van Zon, M. Klee and P. K. Larsen, Integrated Ferroelectrics **3** 283 (1993)
[15] K. Streenivas, Y. Reaney, T. Maerder, N. Setter, C. Jagadish and R. G. Elliman, J. Appl. Phys. **75** 232 (1994).
[16] G. A. C. M. Spierings and P. K. Larsen, 26. IFF Ferienkurs: Elektrokeramische Materialien, C7-1 (1995)
[17] A. Smolenski, V. A. Isupov, A. I. Agranovskaya, Sov. Phys. Solid State **3** 651 (1961)
[18] C. A. Paz de Araujo, J. D. Cuchiaro, M. C. Scott and L. D. Mcmillan, International Patent Publication WO 93/12542, (1993)
[19] Landolt-Bernstein, *Ferroelectric: Oxides*, ed. T. Mitsui and E. Nakamura, Band 16a and 28a, Springer Verlag, Berlin, (1990).
[20] C. A. Paz de Araujo, J. D. Cuchiaro, M. C. Scott and L. D. Mcmillan, International Patent Publication WO 93/12542, (1993)
[21] T. Nakamura. Y. Nakao, A. Kamisawa and H. Takasu, Appl. Phys. Lett. **65** 1522 (1994)
[22] R. A. Roy, K. F. Etzold and J. J. Cuomo, MRS Symp. Proc. **200** 141 (1990).
[23] M. Klee, R. Eusemann, R. Waser, W. Brand and H. van Hal, J. Appl. Phys. **72** 1566 (1992)
[24] M. De Kejiser, P. J. van Veldhoven and G. J. M. Dormans. MRS Symp. Proc. **310** 223 (1990)
[25] A. Ramtrom, Processing details presented at Int. Symp. on Integrated Ferroelectrics (1992)
[26] G. H. Wehner and G. S. Anderson, "*The nature of physical sputtering* in *Handbook of Thin Film Technology,* eds. L. I. Maissel and R. Glang, Mcgraw-Hill NY (1974)
[27] J. Geerk et al; Materials Science Reports 4 193 (1989)
[28] U. Poppe, 26 IFF-Ferienkurs: *Elektrokeramische Materialien* B4 1-38 (1995)
[29] C. L. Jia, J. Rodriguez Contreras, U. Poppe, H. Kohlstedt, R. Waser, and K. Urban; J. Appl. Phys.9 (1) 101 (2002)